Monitoring Networks in Fractured Rocks: A Decision Analysis Approach

by Karen Jardine, Leslie Smith, and Tom Clemo[a]

Abstract

Hydrogeological decision analysis is applied to the design of a performance monitoring network at a waste management facility overlying fractured bedrock. The objective of the monitoring system is to detect contaminants before they reach a regulatory compliance boundary in order to enable early and less costly on-site remediation, and avoid the potentially more costly consequences of failure. Features in the design of the monitoring network include the number of monitoring wells to be installed and their locations, where in each borehole to position discrete monitoring zones, and how often to take water samples. The decision model identifies the preferred monitoring strategy as the design alternative, among all those considered, that minimizes the sum of the monitoring costs and the expected costs of failure and on-site remediation. At a given distance from the facility, the highest probabilities of plume detection are obtained when the fractures intersecting the borehole wall that carry the largest flows are monitored. Monitoring intervals centered on fractures with highest aperture, or regions of highest fracture density, yield intermediate values, while intervals located at predetermined depths yield the lowest probabilities of detection. The monitoring scheme with the highest probability of detection is not necessarily the preferred monitoring strategy. For monitoring options that have a higher probability of detection than the preferred monitoring strategy, the higher expected cost of on-site remediation, when combined with the increased cost of monitoring required to provide the higher probability of detection, can outweigh the reduction in the expected cost of failure brought about by a higher probability of detection. When the probability of contaminants migrating to the compliance boundary is small during the compliance period, changes in the probability of detection brought about by a more intense monitoring effort do not affect the expected cost of failure much; in these instances, the decision model may point to a reduced effort in performance monitoring.

1.0 Introduction

Decision analysis has been described as a formalization of common sense for decision problems which are too complex for informal common sense (Massmann and Freeze, 1987a). It enables one to choose the best alternative from a number of alternative courses of action. Massmann and Freeze (1987b) first illustrated the potential usefulness of a decision framework in the design of a ground-water monitoring system, based on an example involving flow in a heterogeneous porous medium. Meyer et al. (1994) have recently presented a related methodology for designing a monitoring network for plume detection that is based on finding an optimal design that considers three objectives; minimizing the number of monitoring wells, maximizing the probability of detecting a contaminant leak, and minimizing the expected area of contamination at the time of detection. They develop examples based on a two-dimensional areal flow model, and examine the factors influencing tradeoffs between the three design objectives. Our intent in this paper is to illustrate a decision model for evaluating monitoring network designs at waste management facilities that overlie fractured bedrock. Few guidelines currently exist to aid in the design of a monitoring network in a fractured rock setting; hydrogeological decision analysis provides a rational basis to integrate the many factors that must be considered in establishing a cost-effective monitoring network.

A generic case study, developed from the perspective of the owner-operator of a new landfill facility, is used to demonstrate the decision process and to explore the factors influencing network design. A landfill cell is excavated into fractured bedrock (Figure 1). A regulatory compliance monitoring network is located at the compliance boundary. A performance assessment monitoring network is to be installed between the landfill and the

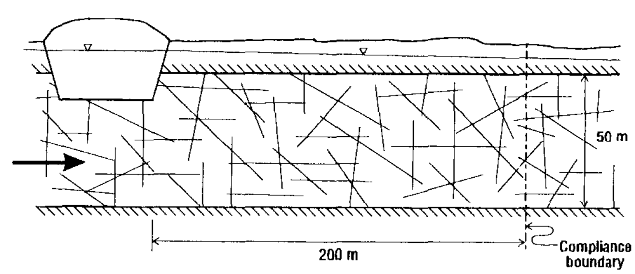

Fig. 1. Schematic cross section for the case study problem.

[a]Department of Geological Sciences, University of British Columbia, 6339 Stores Road, Vancouver, BC, Canada V6T 1Z4.

Received August 1994, revised June 1995, accepted June 1995.

compliance boundary, so that the owner/operator can implement a remedial program before contaminants reach the compliance surface, in the case where contaminants are detected by the monitoring network. Prediction of migration pathways in fractured rocks is subject to considerable uncertainty. The impact of prediction uncertainty is introduced into the network design through a risk term in the decision model. The risk term deals with the consequences of contaminants entering the fractured bedrock. Three possible consequences are considered: (1) contaminants are not detected by the performance monitoring network, but they migrate to the compliance boundary, in which case failure occurs; (2) the contaminant plume is detected and remediated before it can cross the compliance boundary, in which case failure does not occur; and (3) contaminants are not detected by the performance monitoring network but remain within the landfill property boundaries. In the risk term, the costs associated with each of these consequences are multiplied by the probability of that consequence occurring. The probabilities associated with each of these outcomes reflect the interplay of the hydrogeologic characteristics of the site, and the design of the monitoring network. Using a discrete network fracture model and stochastic simulation techniques, we illustrate how the decision framework can guide the planning of a performance monitoring network. For an overview of hydrogeological decision analysis, see papers by Freeze et al. (1990) and Massmann et al. (1991). Meyer et al. (1994) provide a review of the recent literature on network design for monitoring ground-water quality.

2.0 The Decision Model

The heart of the decision model is a risk-cost-benefit analysis of each alternative network design or monitoring strategy. The objective function, equal to the net present value of the risks, costs, and benefits, is given:

$$\Phi = \sum_{t=0}^{T} \frac{1}{(1+i)^t} [B(t) - C(t) - R(t)] \tag{1}$$

where Φ is the objective function (dollars), t is time (years), T is the compliance period, i is the discount rate (decimal), B(t) is the revenue in year t (dollars), C(t) are the costs in year t (dollars), and R(t) are the risks in year t (dollars). When the analysis is carried out from the perspective of the owner/operator, the compliance period is often the expected lifetime of the facility, usually between 10 and 50 years (Massmann and Freeze, 1987a). If the analysis is carried out from the perspective of a regulatory agency, or the owner/operator is required to provide some guarantee against failure after the facility is decommissioned, the compliance period may be extended. The current bank lending rate is usually used for the discount rate (Freeze et al., 1990). Compliance boundaries are usually located closer to a facility than the 200 m used in this study. We locate the compliance boundary well away from the facility to allow for the comparison of monitoring networks placed over a wider range of distances from the contaminant source.

We consider only a performance monitoring network constructed within the property boundaries of the landfill. There is no analysis of the trade-off between facility design and monitoring, or of monitoring at the compliance boundary. We assume that the revenues generated by the landfill would be the same regardless of the monitoring strategy adopted. Thus it is possible to neglect the benefits term. Since the trade-off between facility design and monitoring is not considered, the capital costs of constructing and operating the landfill are also the same regardless of the monitoring strategy chosen. The same holds true of the costs associated with monitoring at the compliance boundary. Consequently, we neglect these costs and consider only those costs directly associated with the construction and operation of the performance monitoring network. These costs are the cost of installing the monitoring network, and the annual cost of monitoring. The cost of installing the monitoring network is the only cost that occurs in year zero, the year before the landfill cell and monitoring system begin operation. With these assumptions, the objective function becomes:

$$\Phi = C_{inst} + \sum_{t=1}^{T} \frac{1}{(1+i)^t} [C_{mon}(t) + R(t)] \tag{2}$$

where C_{inst} is the cost of installing the monitoring network, and C_{mon} is the annual cost of monitoring. The network design/monitoring strategy that provides the minimum value for the objective function, representing the minimum of actual costs plus expected costs, is the preferred alternative.

The risk term represents the expected costs associated with either the detection of contaminants by the performance monitoring network or with failure at the compliance boundary. The costs associated with detection are those incurred in remediating the contamination while it is still within the compliance boundary. The costs of failure can include, for example, regulatory penalties, the cost of litigation, or mandated actions to prevent off-site migration. It is assumed for the purposes of the decision model that an agreement exists between the owner/operator and the regulatory agencies involved that, should contaminants be detected at the compliance boundary, a barrier wall will be constructed around the property boundary to contain the contaminant plume. The barrier wall must be constructed in the year during which detection occurs at the compliance boundary.

For a site with no monitoring network, the risk term is equal to the expected costs associated with failure:

$$R(t) = P_f(t)\, C_f(t) \tag{3}$$

where $P_f(t)$ is the probability of failure in year t, and $C_f(t)$ are the costs that arise as a consequence of failure in year t. For sites with a performance monitoring network, the risk term is expanded to allow for the possibility of the plume being detected and remediated before failure occurs:

$$R(t) = [P_{fm}(t)\, C_{rf}(t)] + [P_d(t)\, C_{rd}(t)] \tag{4}$$

where P_{fm} is the probability of failure in year t with monitoring; $C_{rf}(t)$ is the cost of containment, given failure, in year t; $P_d(t)$ is the probability of detection in year t; and $C_{rd}(t)$ is the cost of early remediation, given detection, in year t. Ongoing costs for operating the remedial system are summed as a separate term, as explained below.

Failure occurs if contaminants reach the compliance surface during the compliance period without being detected by the performance monitoring network. The probability of failure in year t, with monitoring, is

$$P_{fm}(t) = P_{fnm}(t)\, [1 - P_d] \tag{5}$$

where $P_{fnm}(t)$ is the probability of failure in year t without monitoring, and P_d is the total probability of detection over the compliance period. The probability of detection represents the cumulative probability of a plume being detected at any time during the compliance period, before it reaches the compliance surface. This formulation assumes that failure will not occur if the plume is detected in the performance monitoring network; that is, early remediation will be successful. A monitoring network may not detect a contaminant plume if the plume travels through the fracture network along fractures that are not being monitored, if the concentration is below detection levels, or if it passes through a monitored location between the times at which that location is sampled.

There are two components to the cost of early remediation, given detection: (1) the cost of installing the remediation system, and (2) the annual cost of operating this system. The cost of installing the remediation system (C_{rdinst}) is a one time cost that occurs only if a contaminant plume is detected. Therefore, the probability that the remediation system will be installed in any given year is $P_d(t)$, the probability of a plume being detected by the monitoring network in that year. The operating costs for the remediation system (C_{rdop}) are ongoing until the end of the compliance period. The probability that the annual operating cost will be paid in any given year is the probability that a plume has been detected by the monitoring network at any time up to and including the previous year.

Incorporating the definition of the probability of failure with monitoring and the two components of the cost of remediation, along with their respective probabilities, into equation (4), the risk term becomes:

$$R(t) = P_{fnm}(t)\,[1 - P_d]\,C_{rf}(t) + P_d(t)\,C_{rdinst}(t) + \sum_{j=1}^{t-1} P_d(j)\,C_{rdop}(j, t) \qquad (6)$$

where $C_{rdop}(j, t)$ is the cost of operating a remedial system in year t, given detection in a previous year j. The final form of the objective function is:

$$\Phi = C_{inst} + \sum_{t=1}^{T} \frac{1}{(1+i)^t} \Big\{ C_{mon}(t) + P_{fnm}(t)\,[1 - P_d] \cdot C_{rf}(t) + P_d(t)\,C_{rdinst}(t) + \sum_{j=1}^{t-1} P_d(j)\,C_{rdop}(j, t) \Big\} \qquad (7)$$

Monitoring is assumed to continue throughout the entire compliance period, even if a contaminant plume is detected and remediation is implemented. Equation (7) is a general form of the decision model; it applies to facilities located above granular porous media, or those located above fractured media. The interaction between the hydrogeologic setting and the monitoring design enters the decision model through the values determined for the probabilities of plume detection, and failure.

Decision trees provide a simple means of illustrating the structure of the decision process. Figure 2 is an example of a decision tree for a time independent version of the objective function (i.e., the discount rate is equal to zero). For this example, we assume the following probabilities and costs (in millions of dollars): (1) cost of installing the monitoring network, $C_{inst} =$ \$0.1 M, (2) total costs of monitoring, $C_{mon} =$ \$0.9 M, (3) costs associated with failure (confinement), $C_f =$ \$5.0 M, (4) costs associated with detection (remediation), $C_r =$ \$1.0 M, (5) probability of failure (without monitoring), $P_f = 0.8$, and (6) probability of plume detection, $P_d = 0.4$. These probabilities represent the total probability of the respective events occurring within the compliance period.

There are two types of nodes in a decision tree: those that represent decisions (squares), and those that represent events that may occur as a result of those decisions (circles). The probabilities of the potential consequences of each event are recorded above each path leading from an event node. Each path is also labeled within the consequence that it represents. The initial node represents the owner/operator's decision of whether or not to install a performance monitoring network. The first event node on each decision leg represents plume detection; the second event node represents failure. The dollar figure at the end of each terminal path is the value of that portion of the risk term, the expected cost, that is represented by that path.

The decision model identifies the design alternative that minimizes the sum of the actual and expected costs. If the owner/operator decides to install a performance monitoring network, the expected costs equal the probability of the plume being detected (0.4) multiplied by the cost of remediation (\$1.0 M), plus the probability of failure with monitoring (0.48) multiplied by the cost of failure (\$5.0 M). There are no expected costs if the plume is not detected, but failure does not occur. Thus, the expected costs for the decision to monitor are \$2.8 million. If the owner/operator does not install a monitoring network, the expected cost is the probability of failure (0.8) multiplied by the cost of failure (\$5.0 M), or \$4.0 million. The owner/operator's expected costs are higher with a decision not to monitor. The actual costs associated with the decision to monitor are the costs of installing and operating the monitoring system (\$1.0 M). There are no actual costs associated with the decision not to monitor. Therefore, the total value of the objective function for

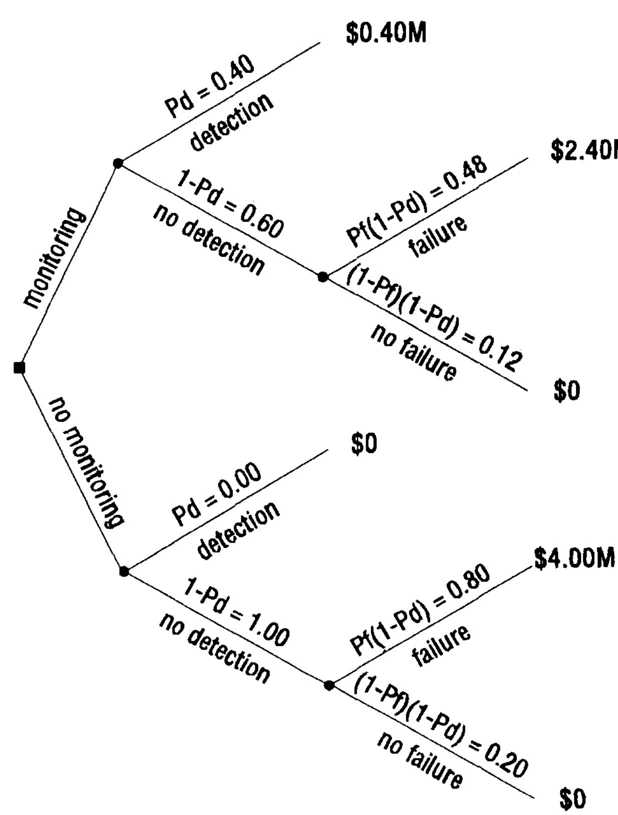

Fig. 2. Decision tree illustrating the structure of the decision model. See text for costs assigned to the various events.

the decision not to monitor is \$4.0 million. For the decision to monitor, the total value of the objective function is \$3.8 million (\$1.0 M + \$2.8 M). Only when the potential savings from detection, which correspond to the reduction in the expected cost of failure, exceed the costs of installing and operating the monitoring network, and the expected costs of early remediation, will the owner/operator consider it worthwhile to install a performance monitoring network. Otherwise, the preferred alternative would be to monitor only at the regulatory compliance boundary, and if contaminants were detected there, to then take on the costs of failure (containment with barrier walls). In this example, although the probability of detection is only 0.4, it is to the owner/operator's advantage to install the monitoring network.

The remediation technique we adopt in the decision model assumes the installation of horizontal interceptor wells at the time when detection occurs. Horizontal interceptor wells would be installed at 50 meter intervals downstream from the contaminant source, up to and including the interval containing the monitoring well at which the plume is detected. Thus, the cost of remediation increases with the distance from the source at which the plume is detected. For simplicity, we assume the remediation system is operated to the end of the compliance period, without regard to the year in which it is installed. To account for the expected costs of operating a remedial system beyond the compliance period, the hydrogeological simulation model would have to be modified to provide an estimate of the time required for restoration of water quality using the horizontal interceptor wells.

A steady-state cross-sectional model is constructed to provide estimates of the probabilities of plume detection and failure on a year-by-year basis. The model domain consists of a rectangular section of fractured rock, with impermeable boundaries along the top and bottom of the domain (Figure 1). The contaminant source is along the upper 10 m of the left boundary, representing the downstream edge of a landfill cell. We have assumed a thickness of 10 m for the upper confining layer, bringing the total depth of the landfill cell to 20 m. The left and right edges of the domain are constant head boundaries, with the right boundary representing the downstream compliance boundary.

Because the model domain is a vertical section, a direct accounting of the effects of the lateral spreading of the plume, and the spacing of monitoring wells perpendicular to the flow direction, is not possible. Computational demands in solving for flow and transport in multiple realizations a three-dimensional fracture model limited us to a two-dimensional analysis. To maintain consistency between the costs of monitoring and the costs associated with detection and failure, it is necessary to devise a pseudo-three-dimensional approach in the decision model. The costs of installing and operating a horizontal interceptor well network, as well as the cost of installing a barrier wall, both assume a three-dimensional geometry; therefore, the cost of performance monitoring should also reflect a three-dimensional geometry. A pseudo-three-dimensional analysis can be established by having each monitoring well represent more than one well in the plane orthogonal to the model plane. We implement this concept by dividing the landfill site into a number of slices, all parallel to the plane of the modeled section. We have arbitrarily chosen to use 10 slices in our examples. Any number of these slices may be monitored, and the cost of monitoring is multiplied by the number of slices to be monitored. Contaminants released from the landfill have an equal chance of entering any slice. The implicit assumption in this approximation is that the contaminant enters and travels in one slice only, consequently detection occurs in only one of the slices. In a practical sense, this implies that lateral dispersion of the plume, given an initial width at the source, does not spread mass beyond the assumed width of the slice. The probability of the contaminant migrating in a slice that is monitored is simply the ratio of the number of slices that are monitored to the total number of slices. The probability of the contaminant being detected is the probability of detection determined in the two-dimensional simulation multiplied by the ratio of the number of slices that are monitored to the total number of slices. The probability of failure with monitoring is also affected by this change in the probability of detection. We assume three monitoring wells are located perpendicular to the direction of ground-water flow (i.e., 3 of 10 slices are monitored). We later investigate the sensitivity of the network design to this three-dimensional approximation.

3.0 Methodology

3.1 Network Design

Key features in the design of the performance monitoring network are: (1) the number of wells to be installed and their locations; (2) where, in each well, to position discrete monitoring zones in relation to the observed properties of the fracture system; and (3) how often to take water samples from the wells. Issues involving the location of monitoring wells center on the distance from the contaminant source to the monitoring wells. One or more discrete monitoring zones are usually isolated within a monitoring well. We assume a 3 meter monitoring zone.

Four criteria for selecting monitoring locations within a well bore are considered: (1) monitoring the fractures along the borehole wall that carry the highest volumetric flows, (2) monitoring the fractures along the borehole wall with the largest apparent apertures, (3) monitoring the areas of densest fracturing, and (4) placing the monitoring loctions at predetermined depths. Information on volumetric flows along a borehole wall could be obtained, for example, from injection tests or a borehole flowmeter survey. The depths of monitoring locations for the predetermined depth monitoring scheme are 16.7, 25.0, and 33.3 m from the top of the fractured rock unit. When one monitoring zone is installed, it is located at 25 m. When two monitoring zones are used, they are installed at 16.7 and 33.3 m. When any of the other monitoring zones are used, they are installed at 16.7 and 33.3 m. When any of the other monitoring schemes are implemented, the monitoring zones are installed hierarchically. For instance, when the highest flow monitoring scheme is implemented and two monitoring zones per well site are required, the monitoring locations are centered about the two fractures carrying the highest flows. The monitoring interval is defined as the period of time between the collection of water samples. In this study, monitoring intervals range from 60 to 360 days. Longer monitoring invervals reduce the annual cost of monitoring, but increase the risk that contaminants go undetected.

3.2 Simulation of Fluid Flow and Contaminant Transport

We adopt a discrete fracture model that simulates flow in a two-dimensional network of planar fractures (Smith and Schwartz, 1993; Clemo, 1994). The rock mass is assumed to be

Table 1. Statistical Properties of Fracture Geometries

Fracture set	Parameter	Base geometry	Geometry 2	Geometry 3
1	Fracture density (m^{-1})	0.35	0.35	0.50
	Mean fracture length (m)	16.0	16.0	5.0
	Mean fracture aperture (m)	20.0E-6	40.0E-6	20.0E-6
	σ log aperture	0.40	0.40	0.60
	Mean fracture orientation (deg.)	0.00	0.00	0.00
	σ orientation (deg.)	10.00	10.00	10.00
2	Fracture density (m^{-1})	0.40	0.40	0.50
	Mean fracture length (m)	4.0	4.0	5.0
	Mean fracture aperture (m)	40.0E-6	40.0E-6	20.0E-6
	σ log aperture	0.60	0.60	0.60
	Mean fracture orientation (deg.)	90.00	90.00	90.00
	σ orientation (deg.)	15.00	15.00	15.00
3	Fracture density (m^{-1})	0.50	0.50	0.50
	Mean fracture length (m)	7.0	7.0	5.0
	Mean fracture aperture (m)	10.0E-6	10.0E-6	20.0E-6
	σ log aperture	0.60	0.60	0.60
	Mean fracture orientation (deg.)	135.00	135.00	135.00
	σ orientation (deg.)	40.00	40.00	40.00

impermeable. Fracture networks are generated by sampling from the statistical distributions that characterize the geometry of the fracture system (e.g., Dershowitz and Einstein, 1988). Fracture length is represented by a negative exponential distribution, fracture aperture by a lognormal distribution, and fracture orientation within a given set by a Gaussian distribution. Fracture density for a fracture set is defined as the number of fractures per meter that are intersected by a line perpendicular to the mean orientation of the fracture set. Six parameters define each fracture set: fracture density; mean fracture length; mean aperture; standard deviation in the log of the apertures; mean orientation of the fracture set; and standard deviation of the orientation. We make the implicit assumption that sufficient data are available to characterize the statistical and hydraulic properties of the fracture system so that the estimated probabilities of failure are a reliable indication of the range of possible site behavior. Note that we do not preserve or condition each of the realizations with measurements on known fractures; nor are the realizations calibrated to hydraulic head or flux data. A discrete network model is used here because it permits an explicit link to be made between the properties of a fracture system, selection of monitoring strategies for locating monitoring zones, and the consequent probabilities of detection. An extensive discussion of issues related to data collection for discrete network models, their strengths and limitations in field studies, and comparisons to other simulation approaches, is available in a report by the National Research Council (1996).

Solute transport is modeled using a particle tracking technique. This method employs a large number of particles to characterize the movement of solute through the flow domain. Particles enter the flow system as an instantaneous pulse. At fracture intersections, mass transfer is modeled using a streamtube routing algorithm (Berkowitz et al., 1994).

The probability of plume detection at each monitoring site is determined by Monte Carlo simulation. The probability of detection is estimated as the number of realizations among a set of 200 realizations in which detection occurred at the well site within the compliance period. Sensitivity studies indicated that 200 realizations were adequate to produce stable results within the decision model.

Monitoring networks are examined for three fracture geometries (Table 1). To organize the presentation, we use geometry 1 as a base case. All three geometries contain three fracture sets: one subhorizontal, one subvertical, and one with a mean orientation 45° counterclockwise from horizontal. In both the base geometry and geometry 2, the subhorizontal fractures are considerably longer than the fractures forming the other two sets. Geometry 2 is similar to the base geometry except that the mean aperture of the subhorizontal fracture set is twice that in the base geometry. In geometry 3, all three fracture sets have the same density, length, and aperture parameters. Representative networks for geometries 1 and 3 are shown in Figure 3a. Note that the vertical lines at regular 25 m intervals are the locations of potential monitoring wells, and not vertical fractures. We have selected the parameter values in Table 1 primarily for the purpose of illustrating a range in hydraulic behavior. While not specific to any site, the values are within the range of values reported in the literature.

Table 2 lists values of the flow and transport characteristics for the three fracture geometries. The effective hydraulic conductivity ranges from 10^{-10} m/s for geometry 3 to 10^{-9} m/s for geometry 2. On average, the networks generated from geometry 2 have an average ground-water velocity almost three times as large as in the base geometry. Fracture networks generated from geometry 3 have an average ground-water velocity that is smaller by a factor greater than five, in comparison to geometry 1.

Figure 3b illustrates the volumetric flows through the fractures in geometries 1 and 3. Although these plots show a single realization, they are representative of the flux distributions in the networks generated from the respective geometries. The line thickness with which each fracture is drawn is proportional to the flow through that fracture. Each plot is scaled to its own maximum flow; consequently, for comparisons between the two geometries, the line widths can be compared only qualitatively. Each fracture network has one or more preferred flow paths which could be expected to act as major conduits for transport.

Table 2. Flow, Transport, and Simulation Parameters for Fracture Systems

Parameter	*Base geometry*	*Geometry 2*	*Geometry 3*
Mean volumetric flow (m^3/day)	1.74E-5	7.43E-5	3.49E-6
Mean travel time of 50th percentile of plume (days)	8,960	3,390	48,020
Mean linear ground-water velocity (m/day)	0.022	0.059	0.004
Mean effective porosity	1.5E-5	2.5E-5	1.7E-5
Number of tracking particles	20,000	32,256	21,510
Length of monitoring interval (days)	60	60	180

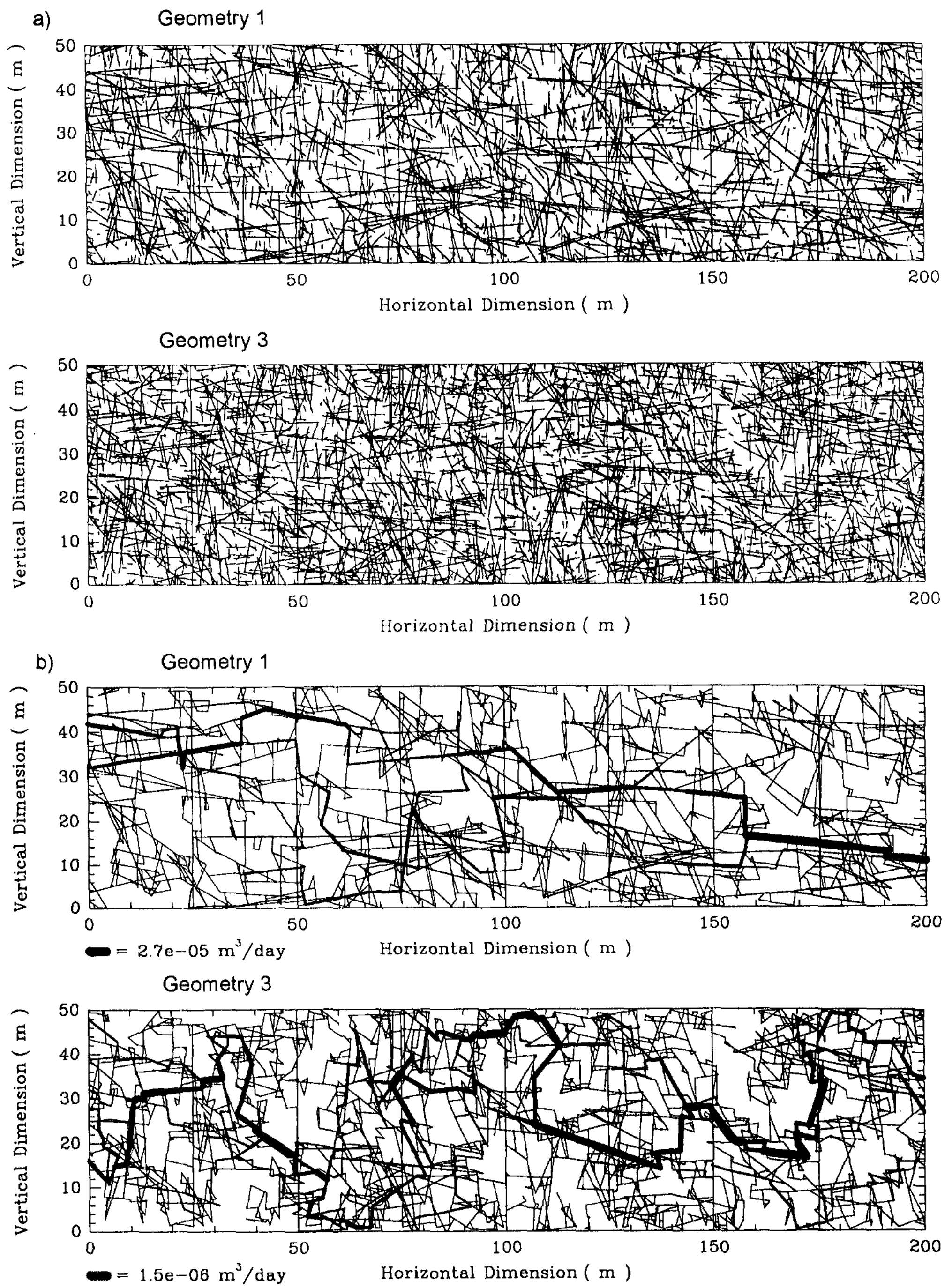

Fig. 3. Examples of fracture networks generated for the base geometry and geometry 3. (a) Fracture patterns, (b) Volumetric flows through each of the networks in (a). Fractures drawn with the narrowest line width carry less than 1/30 of the maximum flow in the network.

3.3 Defining Detection

Detection occurs at the earliest time concentrations at a monitoring location exceeding a detection threshold during a monitoring period. In the simulation model, particles migrating through a monitoring interval under natural gradient conditions are counted over a monitoring period. The length of this monitoring period is arbitrarily set to the travel time for solutes to pass through a sampling volume of radius 0.5 m around the monitoring location (Jardine, 1993). No attempt is made to define absolute concentration values for an indicator species by assigning a quantity of mass to each particle. Rather, the comparison is based on a specific number of particles in a sampling volume that corresponds to the average daily flow through a monitoring location for each fracture system. To calculate the particle concentration, the number of particles that pass through a monitoring location during a monitoring period is divided by the volume of fluid that has flowed through that monitoring location during the monitoring period.

For the base geometry, 20,000 particles are released at the source. This number of particles produces stable transport characteristics. To keep the particle concentration per unit volume constant for the three fracture systems, we adjust the number of particles injected at the source, but retain the same detection threshold concentrations. Unless otherwise stated, the detection threshold concentration is 3.8×10^6 particles/m^3 (corresponding, in the base geometry, to 20 particle per day passing through a monitoring location with the average flow).

3.4 Defining Failure

Failure occurs when contaminants from the landfill cell reach the compliance boundary during the compliance period without being detected by the performance monitoring network. The compliance period is 30 years. The time of failure is calculated as the time at which 0.1% of the mass introduced at the source crosses the compliance surface. The probability of failure without monitoring is estimated as the proportion of realizations among the 200 realizations in which failure occurs during the compliance period. The probability of failure with monitoring is calculated using equation (5). The major assumptions inherent in this definition of failure are that regulatory monitoring at the compliance surface is perfect and failure does not occur if the on-site remedial system is implemented.

3.5 Cost Estimates

Cost estimates used in the decision model, derived from discussions with local and national contractors, are compiled in Table 3. When calculating the costs of installing the monitoring network, we assume a separate borehole is drilled for each monitoring zone at a monitoring site.

Table 3. Decision Analysis Parameters for Base Case

Basic objective function parameters:	
Discount rate (%)	5.0
Compliance period (years)	30.0
Total number of slices in pseudo-three-dimensional domain	10
Number of monitored slices	3
Monitoring cost parameters:	
Advance rate for drilling (m/hr)	5.0
Drill rig chargeout rate ($/hr)	145
Technician chargeout rate ($/hr)	60
Cost of 3 m length of well casing ($)	30
Cost of 3 m length of well screen ($)	50
Cost of 25 l bag of bentonite ($)	35
Cost of 30 l bag of sand ($)	10
Cost per well site of borehole logging ($)	1,000
Cost of collecting, shipping, and analyzing each water sample ($)	525
Costs associated with detection:	
Cost of constructing each interceptor well ($)	500,000
Annual cost of operating each interceptor well ($)	20,000
Costs associated with failure:	
Cost of constructing grout barrier wall ($)	5,000,000

4.0 Results

The cumulative probability of failure for the three fracture geometries we consider is shown in Figure 4. The higher ground-water velocity in geometry 2 is reflected in the probability of failure. During the first 10 years of the compliance period, geometry 2 has a much larger probability of failure than does the base geometry, although the cumulative probabilities of failure are approximately the same by the end of the compliance period. The lower ground-water velocity in geometry 3 is evident from the late failure times and relatively low probability of failure within the compliance period. From the perspective of the likelihood of off-site migration, the base geometry and geometry 2 represent a poor site selection, while geometry 3 is representative of a relatively better site.

4.1 Base Geometry

The probability of plume detection over the compliance period, plotted as a function of the distance of a monitoring well from the landfill cell, is shown in Figure 5. These results are based on one monitoring zone per well site. The highest flow monitoring scheme consistently provides the highest probability of detection, the aperture and density schemes give intermediate values, while the predetermined depth scheme gives the lowest probability of detection. In the predetermined depth scheme, no weight is given to features that potentially indicate higher flux rates and preferred pathways; for this reason, this scheme has the lowest

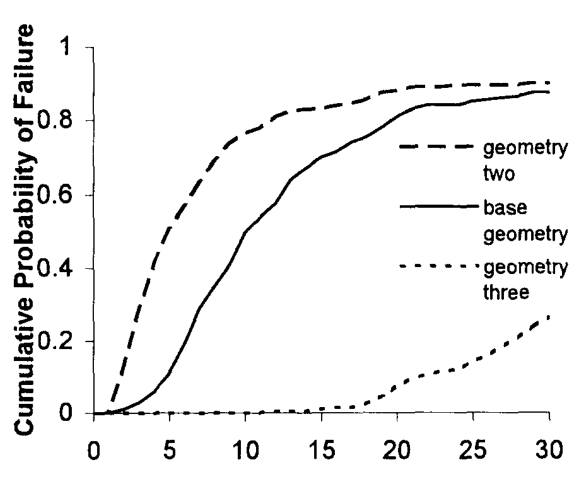

Fig. 4. Cumulative probability of failure for each of the three fracture systems.

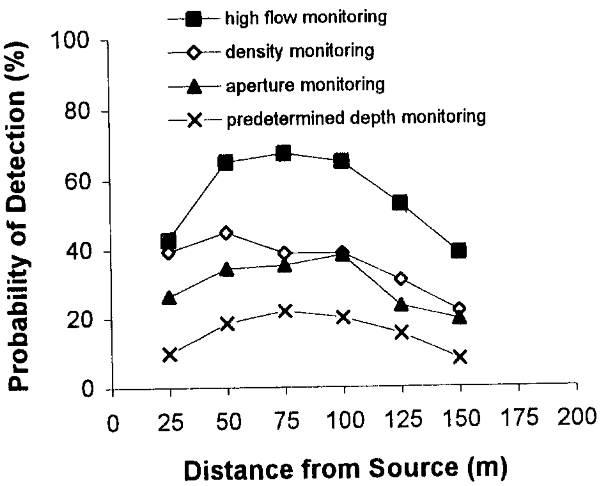

Fig. 5. Probability of detection calculated for a single monitoring well, plotted as a function of the distance of the well from the source. One monitoring zone at the well site. Base geometry.

values for the probability of detection. The differences in the probability of detection between the high flow monitoring scheme and the schemes based on fracture density or aperture occur because there need not be a strong correlation between fluid flux and these geometric properties as observed along a borehole wall. Recall these probabilities of detection apply to a vertical slice that contains a monitoring well. The probability of detection is reduced in magnitude in the decision model, towards values that intuitively seem more appropriate for a three-dimensional domain.

The probabilities of detection are highest approximately 75 m from the source. Probabilities of detection for monitoring wells near the landfill cell are smaller than the peak values because the contaminant, which enters in the top 10 meters of the domain, has not had much opportunity to migrate vertically. For all the monitoring schemes except those based on predetermined depths, a single monitoring location is just as likely to be located in the lower portion of the domain as it is in the upper portion. Thus, near the landfill cell, it is more probable that the bulk of the contaminant is localized in fractures that are not monitored. As the plume moves farther from the source, it is more likely to encounter pathways that transfer solutes towards the base of the fractured unit. This behavior is supported by an examination of the volumetric flow patterns in Figure 3b. As the plume spreads, it is more likely to be travelling in fractures that are monitored, and the probability of detection increases. This behavior is consistent with that reported by Meyer et al. (1994). At greater distances contaminant concentrations may drop below the detection threshold. This dilution is quantified by the particle tracking algorithm and it is reflected in the tailing off of the probabilities of detection at monitoring sites located farther than 100 m from the source.

Our examination of monitoring strategies is not exhaustive; the decision model does not attempt to identify optimal locations for well sites. An alternate strategy for monitoring in the near-source region, suggested on the basis of results in Figure 5, would be to locate a monitoring zone in the upper one-third of the fractured aquifer, centered on the fractures that carry the highest flows within that segment of the aquifer.

Figure 6 compares the probabilities of detection for one, two, and three monitoring zones per well site for the highest flow

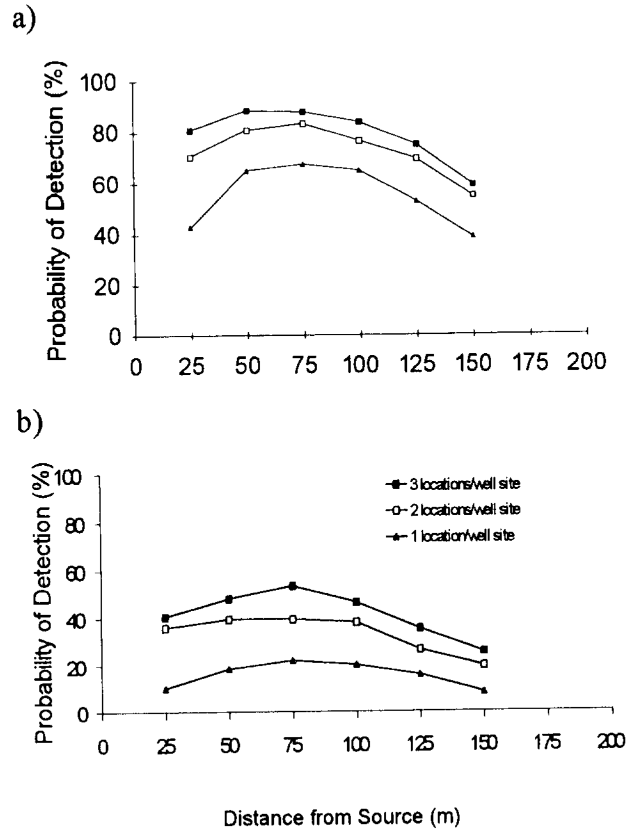

Fig. 6. Probability of detection, using one, two, or three monitoring zones in a single well located at different distances from the source. Base geometry. (a) Highest flow monitoring scheme, (b) Predetermined depth monitoring scheme.

and predetermined depth monitoring schemes. The difference between the probabilities of detection from one to two monitoring zones is greater than the difference from two to three monitoring zones at every well site for each of the four monitoring schemes. The greatest difference in the probability of detection between one and two monitoring zones occurs near the landfill. While the plume is small and likely located in the upper portion of the domain, the chances of detecting contaminants increase much more by the addition of a second monitoring zone at each well site than they do once the plume is more dispersed. Whether the increase in the probability of detection resulting from the installation of additional monitoring locations at any given well site is worth the additional expense of installing and sampling from those monitoring locations is a question that must be evaluated within the decision model.

A histogram of the objective function (Φ) for the base geometry is shown in Figure 7. The long axis of the plot displays four sets of columns, with each set indicating the distance of the monitoring wells from the source (25, 50, 75, or 100 m). Within each set, the three columns record the value of Φ as a function of the number of monitoring zones per well site. For each set, the column closest to the viewer represents the value of Φ with one monitoring zone, the middle column is for two monitoring zones, and the farthest column is for three monitoring zones. The short axis of the histogram plot indicates which of the four monitoring schemes is used to position the monitoring zones within the borehole. Because we only plot the objective function to a distance of 100 m, the effects of dilution seen in Figures 5 and

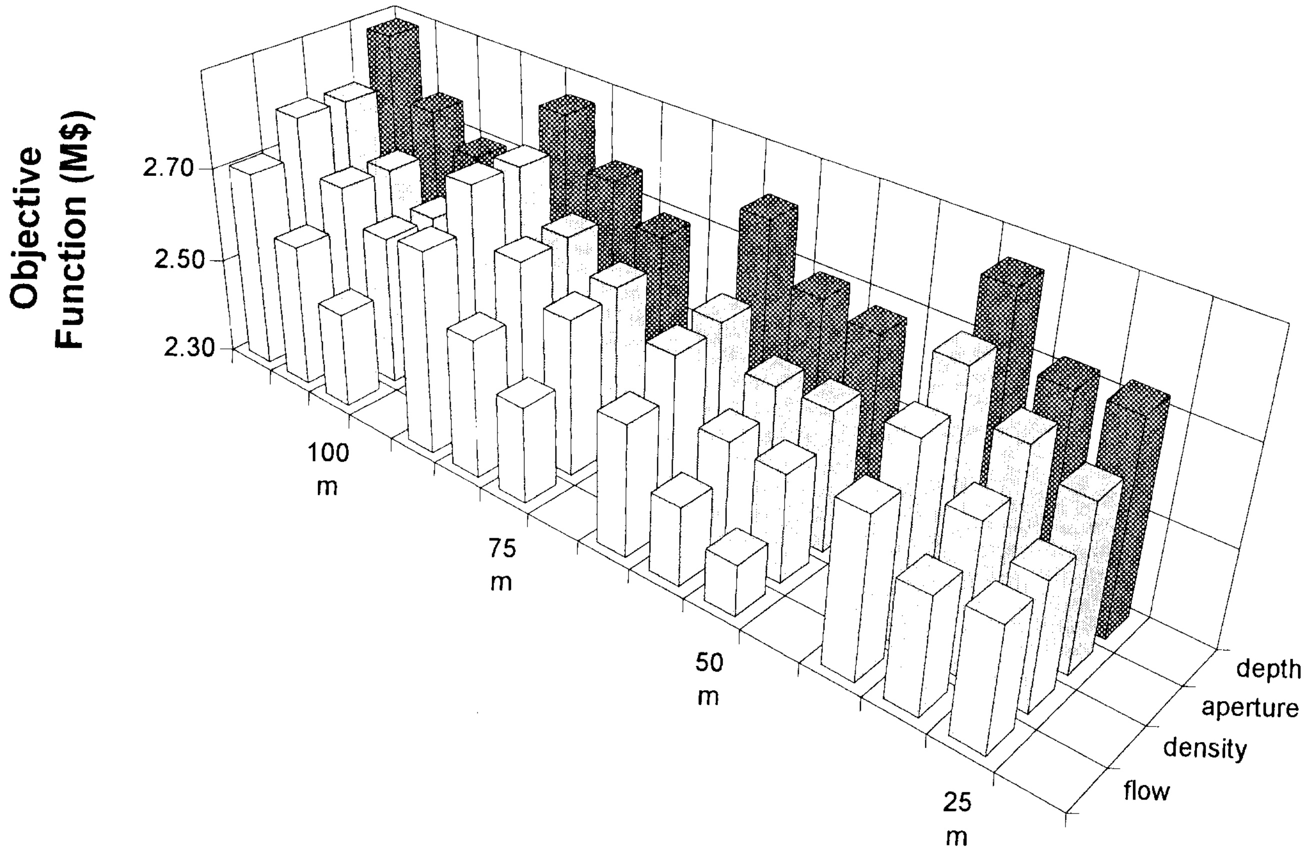

Fig. 7. Values of the objective function for the base geometry. From right to left, each of the sets of three columns at a given monitoring distance corresponds to one, two, and three monitoring zones per well site.

6 do not come into play in a significant way in interpreting Figure 7.

The highest flow monitoring scheme consistently gives the lowest values for Φ, while the predetermined depth scheme gives the highest values. When no performance monitoring is implemented, the value of the objective function is \$2.64 million. The predetermined depth monitoring scheme is the only one that does not provide at least one option with an objective function value lower than this value. When monitoring at predetermined depths, the probability of detection at all well sites is so low that the costs of monitoring are not offset by the reduction in the expected cost of failure afforded by detection.

In almost every instance, one monitoring zone per well site provides a lower value for the objective function than do two or three monitoring zones per well site. The higher values obtained for Φ when more than one monitoring location is installed indicates that the reduction in the expected costs associated with failure, incurred as a result of the increase in the probability of detection, are not as great as the additional expenses incurred in monitoring. The two instances where one monitoring zone per well site does not provide the lowest value of Φ occur at the 25 m well site when either the highest flow or the predetermined depth monitoring scheme is implemented. In these instances, the difference in the probability of detection between one and two monitoring zones is considerably larger than in any of the other situations. In these cases the reduction in the expected costs of failure outweigh the increase in both the costs associated with monitoring and the expected costs associated with early remediation.

The lowest value for the objective function, \$2.41 million, occurs at a well site 50 m from the source, with one monitoring zone centered about the fracture carrying the highest flow. This is not the monitoring scheme that provides the highest probability of detection. The highest probability of detection occurs with the flow monitoring scheme at the well site located 50 m from the source with three monitoring zones installed. When only one monitoring zone is installed per well site, the highest probability of detection occurs at the well site located 75 m from the source. This monitoring scheme does not provide the lowest value of the objective function, however, because two horizontal interceptor wells are required for the remediation program if detection occurs at 75 m. Any advantage gained by the higher probability of detection at 75 m is offset by the additional expected cost of installing and operating two interceptor wells.

A number of sensitivity studies involving both monitoring parameters and decision parameters are carried out using the base geometry. Unless otherwise indicated, the results presented are those obtained when the highest flow monitoring scheme is implemented, with one monitoring zone at the well site.

Detection Threshold: The probability of detection, for three different detection thresholds, is shown in Figure 8. Lower detection thresholds lead to higher probabilities of detection. When no dilution effects are considered (i.e., a detection threshold of one particle per monitoring period), the probability of detection increases to a distance of 125 m from the source, where it levels off. This steady rise reflects the increasing likelihood, as the plume disperses, that contaminants will be transported in fractures that are monitored. Values of the objective function

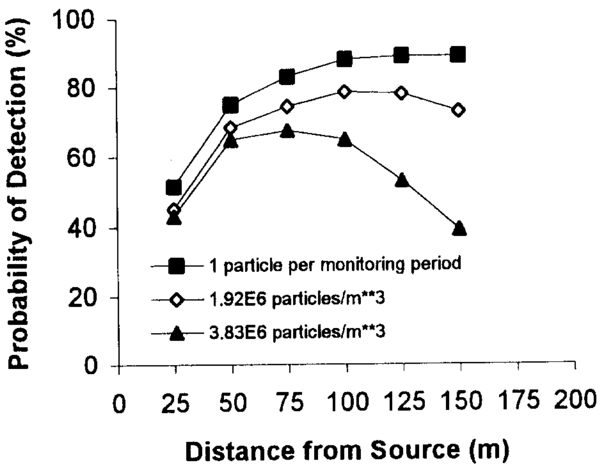

Fig. 8. Probability of detection for the base geometry, for different detection thresholds.

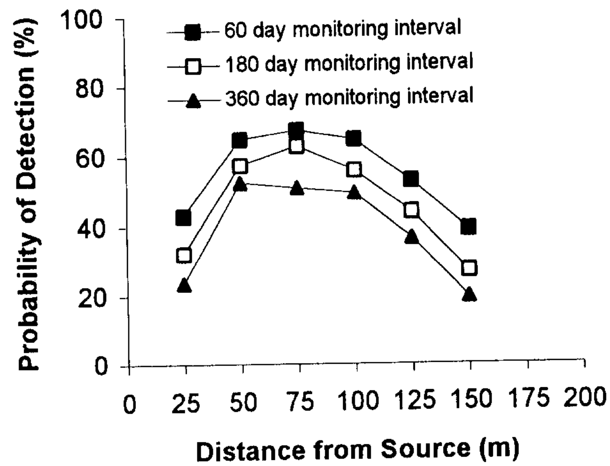

Fig. 9. Probability of detection for the base geometry, for different monitoring intervals.

decrease with a smaller detection threshold because the reduction in the expected cost of failure brought about by the increased probability of detection outweighs the consequent increase in the expected cost of early remediation. In general, however, the differences in Φ are less between detection thresholds than they are between different numbers of monitoring locations, or monitoring locations at different distances from the source.

Monitoring Interval: Three monitoring intervals are compared; 60, 180, and 360 days. The probability of detection decreases as the monitoring interval increases (Figure 9). With a pulse input of mass, and the many different pathways that can be taken from the landfill cell to each of the monitoring locations, there is a wide variation in the amount of contaminant that passes through a monitoring location from one monitoring period to another. The less frequently a sample is taken, the lower the probability that a sample will be taken during a monitoring period when the contaminant concentration is large enough to constitute detection. This behavior is probably exaggerated to some extent by the discrete nature of the particle tracking procedure. In the simulations with no detection threshold, the probability of detection is less sensitive to the monitoring interval. The same pattern is evident, however, with a smaller probability of detection at the longer monitoring interval.

With a few exceptions, the value of the objective function decreases as the length of the monitoring interval increases, reflecting the lower cost of monitoring associated with less frequent sampling (Figure 10). When one monitoring zone is installed 25 m from the landfill cell, the value of Φ increases when the monitoring interval is lengthened from 180 to 360 days. This

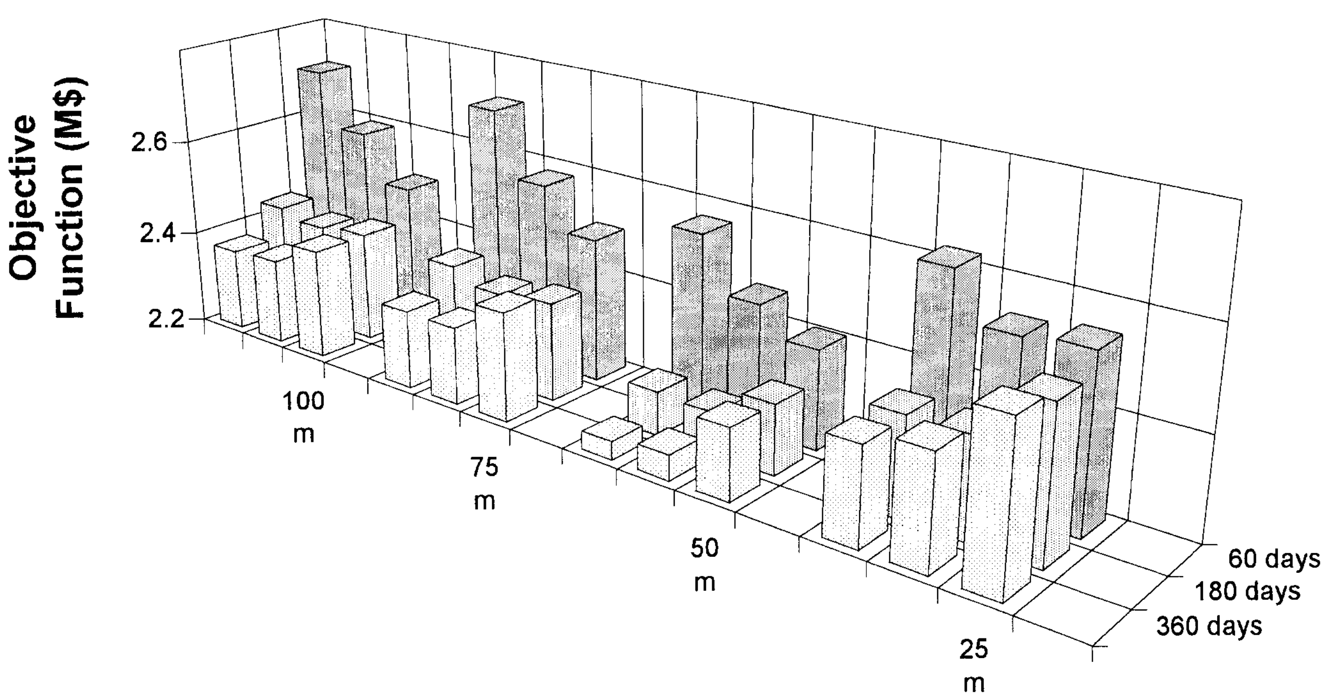

Fig. 10. Values of the objective function for different monitoring intervals, base geometry. From right to left, each of the sets of three columns at a given monitoring distance corresponds to one, two, and three monitoring zones per well site.

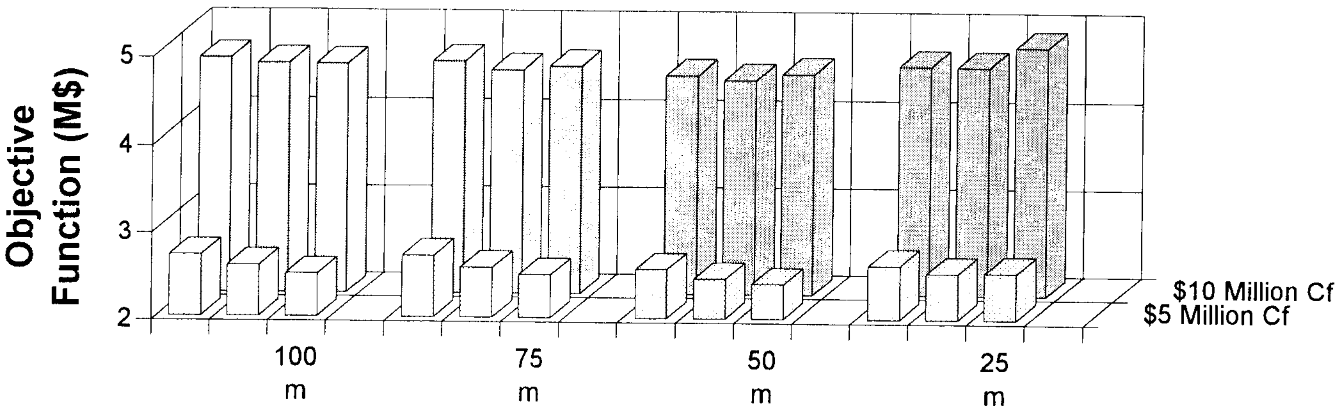

Fig. 11. Values of the objective function for two different costs of failure, base geometry. From right to left, each of the sets of three columns at a given monitoring distance corresponds to one, two, and three monitoring zones per well site.

increase indicates that the reduction in monitoring costs afforded by the drop in sampling frequency is smaller than the increase in the expected costs brought about by the decrease in the probability of detection. As the monitoring interval increases, the lowest value for Φ shifts to designs where more than one monitoring zone is installed at each well site. When the monitoring interval is 180 days, the lowest value for Φ at each well site occurs when there are two monitoring zones. When the monitoring interval is increased to 360 days, the lowest value for Φ at three of the four well sites shown occurs when there are three monitoring zones. With less frequent sampling, the ongoing costs of sampling are reduced to the point that the increased monitoring costs incurred by the addition of monitoring locations are outweighed by the reduction in the expected costs that result from the increased probability of detection that accompanies the addition of monitoring zones. Not considered in this analysis are the potentially higher costs of on-site remediation if the plume migrates a substantial distance beyond the performance monitoring wells between sampling rounds. These histograms are a good illustration of the way in which the decision model can resolve complex design issues in a straightforward fashion. Figure 10 suggests that for this scenario, the favored performance monitoring strategy involves less frequent sampling at more monitoring zones, rather than fewer monitoring zones sampled more frequently.

Discount Rate: The higher the discount rate, the smaller the impact of the actual and expected costs that are incurred in later years, and the larger the impact of the initial cost of constructing the monitoring system. Values of the objective function obtained with a discount rate of 10% are less than half those when the costs are not discounted over time. Other than changing the absolute value of the objective function, however, changing the discount rate in the range from 0 to 10% does not have a significant impact on the network design for the base geometry.

Cost of Failure: Increasing the cost associated with detection at the compliance boundary places more weight on the expected cost of failure relative to the actual monitoring costs. Additional costs incurred to provide an increase in the probability of detection may be offset by the reduction in the expected cost of failure. For the base case, when the cost associated with failure is $5 million, the lowest value of the objective function is usually obtained with one monitoring zone installed per well site. If the cost of failure is doubled to $10 million, the lowest value for Φ at each well site occurs when two monitoring zones are installed (Figure 11). With the larger cost associated with failure, the reduction in the expected cost of failure provided by an increase in the probability of detection is large enough to offset the increased costs incurred when two monitoring zones are installed, but not those incurred when three monitoring zones are installed.

Pseudo-Three-Dimensional Analysis: The pseudo-three-dimensional calculation in the decision model is an attempt to maintain consistency between the costs of monitoring and the expected costs associated with detection and failure. The histograms in Figure 12 compare a two-dimensional analysis, the base case in which three of 10 slices are monitored, and an analysis in which the site is represented by 20 slices, three of which are monitored. The values of the objective function with the two-dimensional analysis are lower because the costs of installing and sampling from additional monitoring wells are one-third of those in the three-dimensional base case, while the probabilities of detection are 3.3 times larger. This difference leads to the behavior where, in the two-dimensional calculation, the lowest value of the objective function at each well site occurs when three monitoring zones are installed, while in the three-dimensional calculations, the lowest value usually occurs when one monitoring zone is installed. In representing the site with a greater number of slices, the probability of detection in the decision model is one-half of that in the base case. The costs of monitoring are the same (three slices are monitored). The smaller probability of detection leads to an increase in the expected cost of failure, giving the higher values for the objective function. However, the identification of the best design among the alternatives considered here is unchanged.

Multiple Well Configurations: A row of monitoring wells situated farther from the source can act as a backup system to detect plumes that may be missed by a closer row of wells. Two multiple well configurations are considered: one with well sites located 25 m and 50 m from the source, and one with well sites at 25 m and 75 m. Figure 13 shows the cumulative probability of detection for the well configurations at 25 and 75 m, with one monitoring zone installed at each well site. The probability of detection for the multiple well configuration is higher than for either of the individual well sites, but not as great as the sum of the two (in some of the realizations plumes are detected at both well sites).

The values for the objective function obtained with both

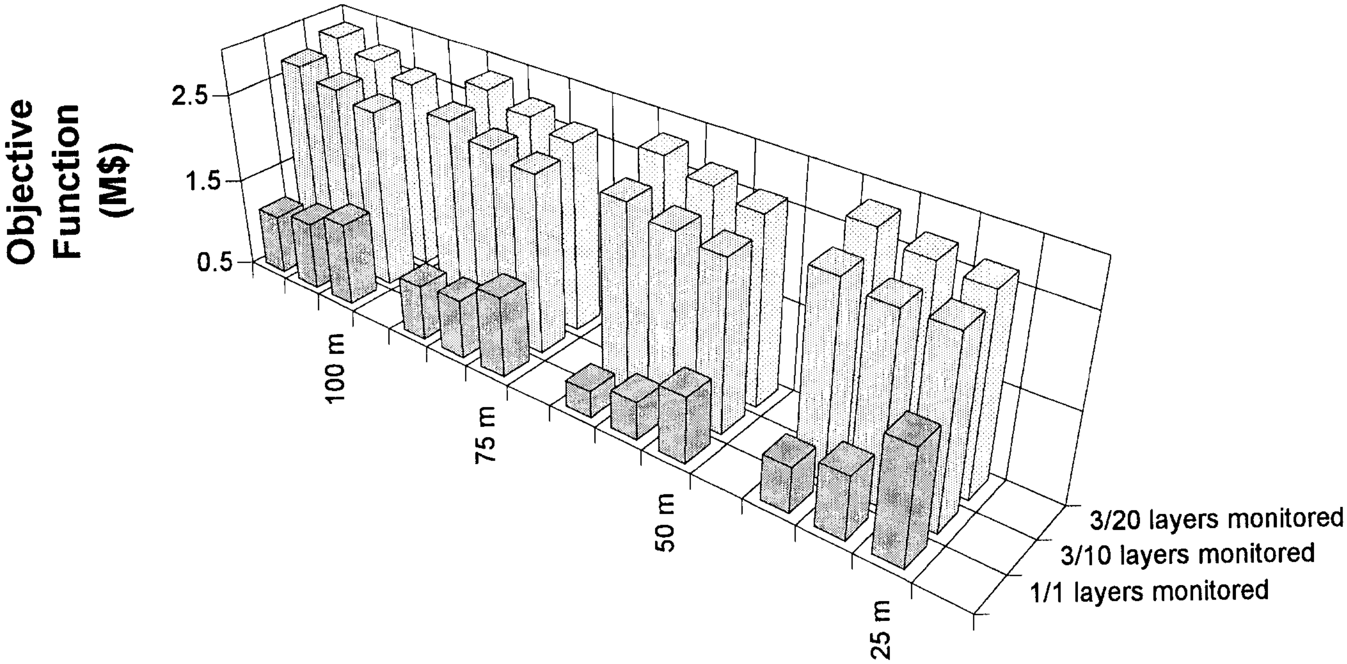

Fig. 12. Values of the objective function for a two-dimensional interpretation of the decision model, and two different pseudo-three-dimensional models, base geometry. From right to left, each of the sets of three columns at a given monitoring distance corresponds to one, two, and three monitoring zones per well site.

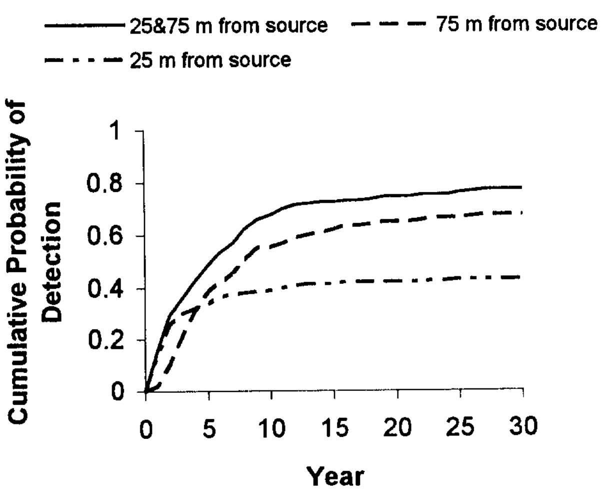

Fig. 13. Probabilities of detection for the base geometry as a function of time, for monitoring wells 25 m from the source, 75 m from the source, and a multiple well configuration with wells at 25 and 75 m.

multiple well configurations are larger than the values obtained at any of the individual well sites (Figure 14). The reduction in the expected cost of failure provided by a higher probability of detection is not sufficient to outweigh the costs of installing and sampling from additional monitoring wells plus the increased expected cost of remediation. Even when the cost of failure is doubled to $10 million, the single well configurations provide lower values for the objective function than do either of the multiple well configurations. The lowest values for the objective function for the multiple well configurations occur when one monitoring zone is installed at each well site. For the scenario evaluated here, the calculations indicate no economic advantage to the incorporation of backup wells in the performance monitoring network.

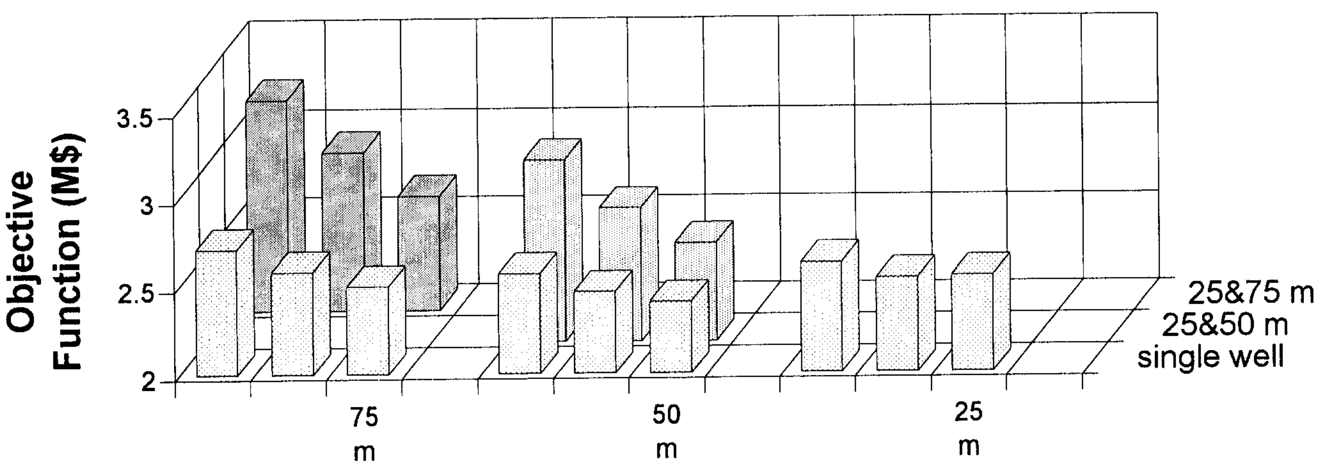

Fig. 14. Values of the objective function for multiple-well configurations. Base geometry. From right to left, each of the sets of three columns at a given monitoring distance corresponds to one, two, and three monitoring zones per well site.

4.2 Geometry 2

Geometry 2 is a scenario where, in the absence of a performance monitoring network, there is a high likelihood of failure early in the compliance period (Figure 4). The fracture system is similar to the base geometry, except that the mean aperture of the horizontal fracture set is twice that of the base geometry. The net present value of the expected cost of failure is higher with early failure because of the effects of discounting with time. Furthermore, given the assumption that the remedial system remains in operation from the time of detection until the end of the compliance period, early detection leads to higher expected costs of remediation.

As in the base geometry, the highest flow monitoring scheme consistently provides the lowest values for the objective function, while the predetermined depths scheme provides the highest values (Figure 15). When no monitoring is undertaken, the value of the objective function is \$3.48 million, almost one million dollars higher than in the base geometry. The predetermined depth monitoring scheme is the only monitoring scheme that does not provide at least one option with an objective function value lower than the value obtained when no monitoring is undertaken. In all but five instances, the lowest value for the objective function occurs when there is one monitoring zone. In the other five instances, there is a substantial increase in the probability of detection when a second monitoring zone is installed, leading to a lower value of Φ in those cases. As seen earlier in the base geometry, the options that provide the highest probabilities of detection do not necessarily provide the lowest value for the objective function. The lowest value obtained for the objective function for geometry 2 occurs at the well site 50 m from the source when the highest flow monitoring scheme is implemented and two monitoring zones are installed at this well site. The decision model points to a more intensive performance monitoring effort for geometry 2, in comparison to geometry 1.

4.3 Geometry 3

Geometry 3 represents better site conditions than either of the other two fracture geometries we consider. Although more densely fractured, geometry 3 does not contain long horizontal fractures (Table 1). Consequently, the effective hydraulic conductivity of the fracture system is reduced in comparison to the base case, and the average ground-water velocity is smaller by a factor of approximately five. The probability of failure during the compliance period is much lower for this fracture geometry and failure occurs later (Figure 4).

There are two differences worth noting in comparing probabilities of detection for this geometry, with those for the base geometry. First, the highest probability of detection occurs closer to the landfill cell than in the base geometry. Figure 3b suggests that the preferred flow paths for geometry 3 are more tortuous than those in the other geometries. The contaminant plume is more likely to have undergone substantial vertical spreading by the time it has travelled 25 m from the contaminant source. Second, the probability of detection falls off at monitoring well sites located beyond 75 m from the landfill cell because in many of the realizations, the plume has not yet arrived at these sites by the end of the compliance period.

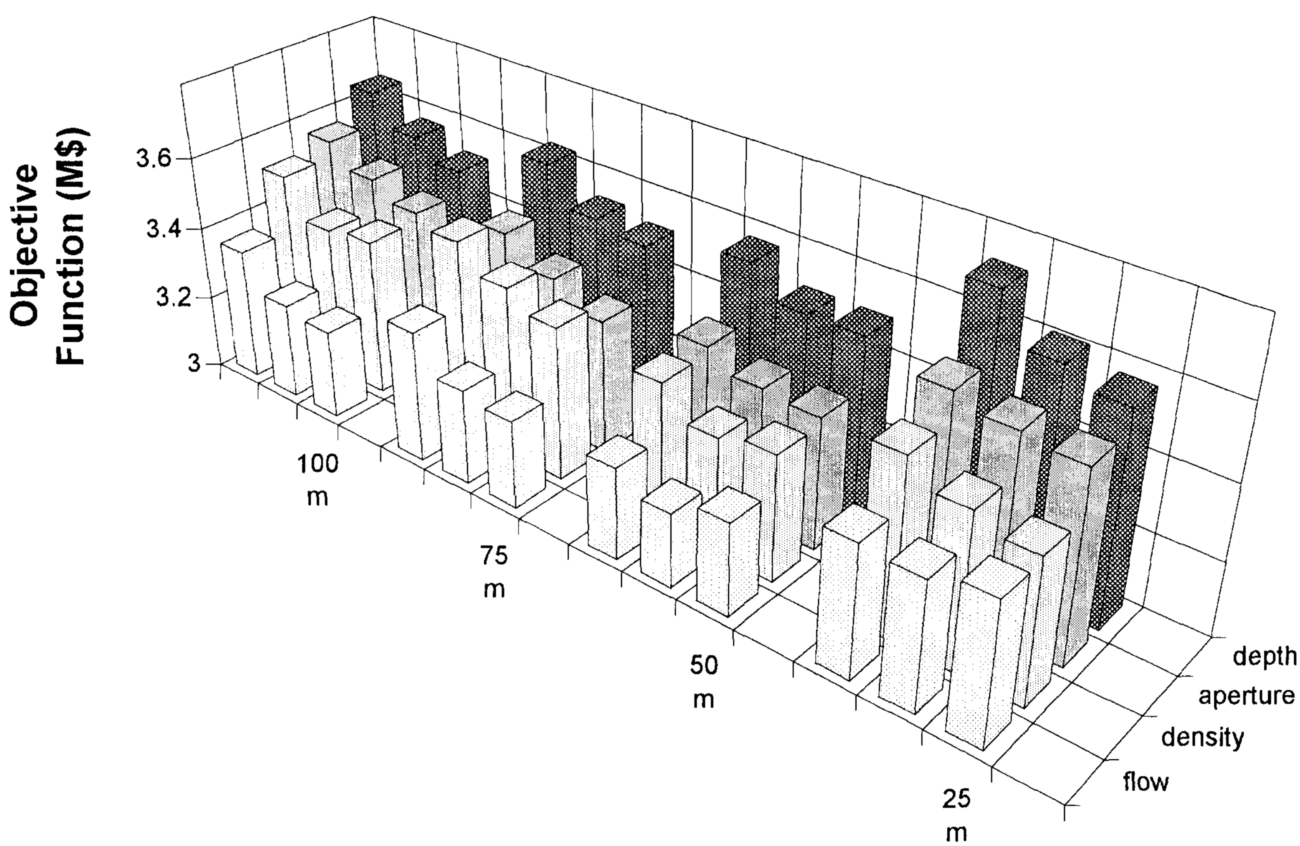

Fig. 15. Values of the objective function for fracture system 2. From right to left, each of the sets of three columns at a given monitoring distance corresponds to one, two, and three monitoring zones per well site.

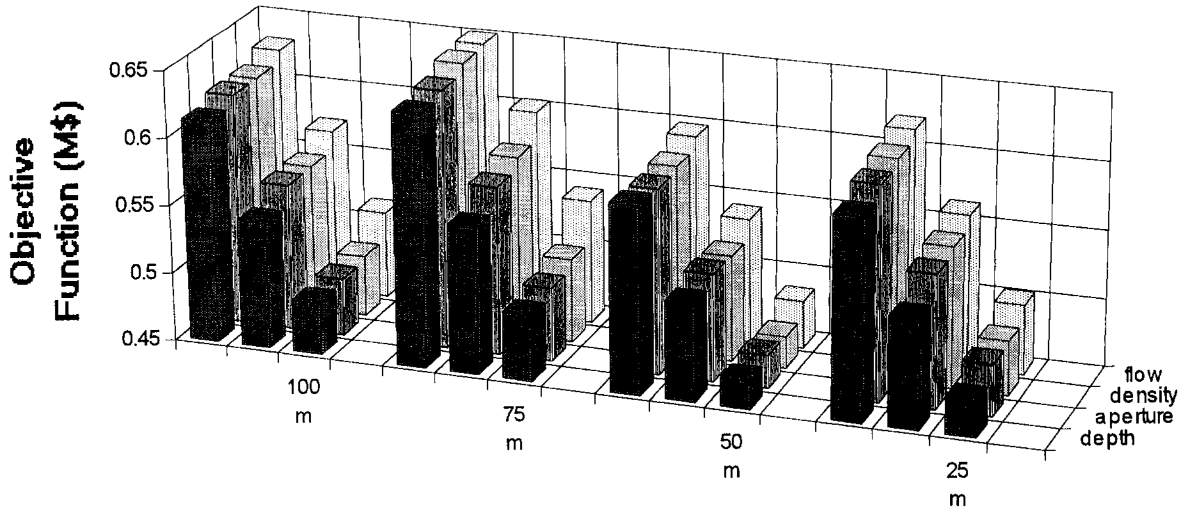

Fig. 16. Values of the objective function for fracture system 3. From right to left, each of the sets of three columns at a given monitoring distance corresponds to one, two, and three monitoring zones per well site.

The behavior of the objective function is quite different for geometry 3, when compared to the earlier two cases (Figure 16). The predetermined depth monitoring scheme consistently provides the lowest values for Φ, followed by the largest aperture, densest fracturing, and highest flow monitoring schemes, respectively. This is the reverse order of monitoring schemes in the other two geometries. As a consequence of the low probability of failure, the objective function is dominated by the cost of monitoring and the expected cost of early remediation. The monitoring scheme that provides the highest probability of detection provides the highest values for the objective function. When no performance monitoring is undertaken, the value obtained for the objective function is $0.42 million, which is lower than any value in Figure 16. Because of the reduced permeability of the fracture system, the probability of off-site migration is low, and the reduction in expected cost of failure provided by performance monitoring is overshadowed by the cost of monitoring and the expected cost of early remediation, for all the alternative designs considered here. Thus, rather than taking on the costs associated with performance monitoring, it would be to the advantage of the owner/operator to rely on the regulatory agreement that a containment system would be installed at the compliance boundary, should contaminants reach there during the compliance period.

Increasing the cost associated with failure will give more weight to the expected cost of failure by increasing the reduction in the expected cost of failure that results from an increase in the probability of detection. When the costs associated with failure are doubled, from $5 million to $10 million, the highest flow monitoring scheme provides the lowest value for the objective function at the two well sites closest to the contaminant source. This value, $0.81 million, is now lower than the value that is obtained when no performance monitoring is undertaken ($0.84 million). With a higher expected cost of failure, network designs can be identified where it is again to the advantage of the owner/operator to install a performance monitoring network.

5.0 Conclusions

Hydrogeological decision analysis can provide a rational basis for an owner/operator to integrate many of the factors that must be considered in designing a performance monitoring network at a waste management facility that overlies fractured bedrock. The decision model identifies the design alternative among all those considered that minimizes the sum of the actual and expected costs. The actual costs are those of installing and operating a monitoring network; the expected costs depend upon the probability of failure during the compliance period, the likelihood of plume detection by the monitoring network, and the costs tied to on-site remediation and the consequences of off-site migration.

In the region near the contaminant source, the probability of detection is sensitive to the rate of vertical spreading through the fracture network. Fracture geometries leading to preferred flow paths that are more tortuous are associated with higher probabilities of detection. The highest probabilities of detection are obtained when the fractures intersecting the borehole wall that carry the largest flows are monitored. Monitoring zones centered on the fractures with highest aperture, or regions of highest fracture density, yield intermediate values for the probability of detection. Monitoring zones located at predetermined depths yield the lowest probabilities of detection. The additional expense of injection tests or a borehole flowmeter survey may be justified if it contributes to a significant reduction in the expected cost of failure.

When considering issues related to the location of monitoring wells, the number of monitoring zones at a given well location, or sampling frequency, the monitoring scheme that provides the highest probability of detection is not necessarily the preferred monitoring strategy. For monitoring options that have a higher probability of detection than the preferred monitoring strategy, the higher expected cost of remediation, when combined with the increased cost of monitoring that may be required to provide the higher probability of detection, can outweigh the reduction in the expected cost of failure brought about by a higher probability of detection.

Our results support a general conclusion reached by Meyer et al. (1994) using a different design framework. Their analyses suggested that emphasizing detection at the expense of a larger plume at the time of detection (i.e., placing the wells further from the source to increase the probability of detection) is an appropriate strategy when the costs of dealing with an undetected release (failure in our examples) are much greater than those involved in dealing with a detected release (early remediation in our examples). For sites with a high probability of off-site migration during the compliance period, the decision model is dominated by the expected cost of failure. Therefore, the cost of failure is also a potential administrative tool available to regulators who wish to promote the use of more conservative performance monitoring networks. When the probability of off-site migration is small during the compliance period, changes in the probability of detection brought about by a more intense monitoring effort do not affect the expected cost of failure much; changes in the expected cost of detection related to on-site remediation can exceed the changes in the expected cost of failure. In these instances, the decision model may point to a reduced effort in performance monitoring.

Acknowledgments

This research was funded by grants from the Natural Sciences and Engineering Research Council of Canada.

References

Berkowitz, B., C. Naumann, and L. Smith. 1994. Mass transfer at fracture intersections: An evaluation of mixing models. Water Resour. Res. v. 30, no. 6, pp. 1765-1773.

Clemo, T. 1994. Dual permeability modeling of fractured media. Ph.D. thesis, Univ. of British Columbia, Vancouver, BC. 279 pp.

Dershowitz, W. and H. Einstein. 1988. Characterizing rock joint geometry with joint system models. Rock Mechanics and Rock Engineering. v. 21.

Freeze, R. A., J. W. Massmann, L. Smith, T. Sperling, and B. James. 1990. Hydrogeological decision analysis, 1: A framework. Ground Water. v. 28, pp. 738-766.

Jardine, K. 1993. Hydrogeological decision analysis: Monitoring networks for fractured geologic media. M.A.Sc. thesis, Univ. of British Columbia, Vancouver, BC. 97 pp.

Massmann, J. W. and R. A. Freeze. 1987a. Groundwater contamination from waste management sites: The interaction between risk-based engineering design and regulatory policy, 1. Methodology. Water Resour. Res. v. 23, pp. 351-367.

Massmann, J. W. and R. A. Freeze. 1987b. Groundwater contamination from waste management sites: The interaction between risk-based engineering design and regulatory policy, 2. Results. Water Resour. Res. v. 23, pp. 368-380.

Massmann, J. W., R. A. Freeze, L. Smith, T. Sperling, and B. James. 1991. Hydrogeological decision analysis, 2: Applications to ground-water contamination. Ground Water. v. 29, pp. 536-548.

Meyer, P. D., A. J. Valocchi, and J. W. Eheart. 1994. Monitoring network design to provide initial detection of groundwater contamination. Water Resour. Res. v. 30, no. 9, pp. 2647-2659.

National Research Council. 1996. Rock Fractures and Fluid Flow: Contemporary Understanding and Applications. National Academy Press, Washington, DC.

Smith, L. and F. W. Schwartz. 1993. Solute transport through fracture networks. In: Flow and Contaminant Transport in Fractured Rocks, ed. by J. Bear, C. F. Tsang, and G. de Marsily. Academic Press.
